Cation Distribution Study of Chromium Substituted Copper Nickel Zinc Ferrite

B. L. SHINDE [1], K. S. LOHAR [2*]

[1] Department of Chemistry, Waghire College, Saswad, Dist: Pune, 412301 (M.S.) India
[2] Department of Chemistry, Shrikrishna Mahavidyalaya, Gunjoti, Dist: Osmanabad, 413606, (M.S.) India
Corresponding Author E-Mail : kslohar@rediffmail.com

Abstract

$Cu_{0.2}Ni_{0.2}Zn_{0.6}Fe_{2-x}Cr_xO_4$ ferrites with composition (x = 0.0, 0.2, 0.4, 0.6, 0.8 and 1.0) synthesized by the sol-gel auto-combustion method. The Bertaut method used to determine the cation distribution. Zn^{2+} ions prefer to occupy the tetrahedron site (A sublattice) and both Ni^{2+} and Cu^{2+} ions mainly enter octahedron site (B sublattice). However, Fe^{3+} ions occupy both the available tetrahedral (A) and octahedral [B] sublattices. With increasing Cr^{3+} content, the fraction Cr^{3+} ions in octahedral sites increases, whereas the fraction of Fe^{3+} ions in octahedral sites decreases linearly.

Keywords: Ferrite, XRD, SEM, Cation distribution.

Introduction

Nanoscience and Nanotechnology is the technology dealing with both single nanoobjects and materials, and devices based on them, and with processes that take place in the nanometer range. Ferrites are chemical compounds, ceramic with iron (III) oxide Fe_2O_3 as their principal components [1]. Ferrites are usually non-conductive ferrimagnetic ceramic compounds derived from iron oxides such as hematite (Fe_2O_3) or magnetite (Fe_3O_4) as well as oxides of other metals. Ferrites are, like most other ceramics, hard and brittle. Many of them are magnetic materials and they are used to make permanent magnets, ferrite cores for transformers, and in various other applications. Many ferrites are spinels with the formula AB_2O_4, where A and B represent various metal cations, usually including iron. Spinel ferrites usually adopt a crystal motif consisting of cubic close-packed (fcc) oxides (O^{2-}) with A cations occupying one eighth of the tetrahedral holes and B cations occupying half of the octahedral holes-that is, the inverse spinel structure.

The site occupancy is often depicted in the chemical formula as $(M_{1-\delta}Fe_\delta)[M_\delta Fe_{2-\delta}]O_4$, where round and square brackets denote the A- and B-sites, respectively, M represents a metal cation, and 'δ' is the inversion parameter. The degree of inversion 'δ' for spinel ferrites are defined as the fraction of tetrahedral (A)-sites occupied by trivalent cations. Accordingly, for a normal spinel δ = 0 and for a completely inverse spinel, δ = 1. The magnetic and the electronic properties of such a ferrite system depend upon the type of metal cations and their distribution among the two interstitial sites, that is, A- and B-sites. Therefore, the knowledge of cation distribution is essential to understand the magnetic behavior of spinel ferrites. Manganese ferrite is early known to be a mixed inverse spinel, and the degree of inversion mainly depends upon the method of preparation. The presence of nonmagnetic ions in these spinel ferrites is found to alter their magnetic and electronic properties. The addition of metal cations such as trivalent or tetravalent influences the electronic and magnetic properties of the ferrite system [2–9].

In the present paper, we presented cation distribution study of $Cu_{0.2}Ni_{0.2}Zn_{0.6}Fe_{2-x}Cr_xO_4$ ferrites with composition (x = 0.0, 0.2, 0.4, 0.6, 0.8 and 1.0).

Experimental

$Cu_{0.2}Ni_{0.2}Zn_{0.6}Fe_{2-x}Cr_xO_4$ ferrites with composition (x = 0.0, 0.2, 0.4, 0.6, 0.8 and 1.0) were synthesized by the sol-gel auto-combustion method from analytical reagent grade nickel nitrate, copper nitrate, zinc nitrate, chromium nitrate and iron nitrate and citric acid as a fuel [10]. The synthesized precursors were calcinated at 500 °C for 4 h to obtain the final product. The composition was determined by energy dispersive X-ray spectroscopy (EDAX, Inca Oxford). X-ray powder diffraction studied by Phillips X-ray diffractometer (Model 3710). Morphology of the powder samples were studied on JEOL-JSM-5600 N Scanning Electron Microscope. The infrared spectra of all the samples were recorded in the range 300 to 800 cm^{-1} using Perkin Elmer infrared spectrophotometer. Morphology of the powder samples were studied on JEOL-JSM-5600 N Scanning Electron Microscope (SEM) and on Philips (model CM 200) Transmission Electron Microscope (TEM).

Results and Discussion

EDAX

A typical EDAX pattern of the chromium substituted copper nickel zinc ferrite system is shown in Figure 1. The EDAX pattern confirmed stoichiometry of the prepared chromium substituted copper nickel zinc ferrite samples was in desired composition.
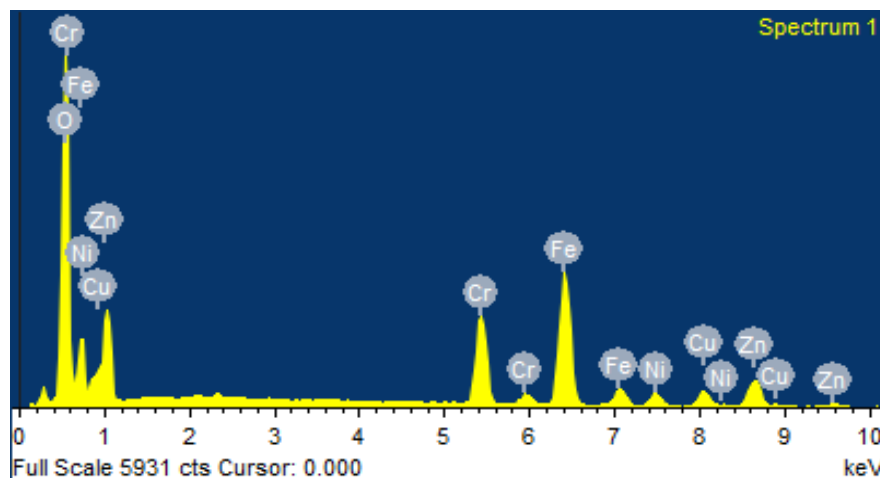

Fig. 1: Typical EDAX pattern for samples x =0.2

X-ray Diffraction

Typical X-ray diffraction (XRD) patterns of the chromium substituted copper nickel zinc ferrite system are shown in Figure 2. The XRD patterns confirmed the formation of cubic spinel structure of single phase ferrites. Lattice constant (a) of all the samples was determined [10], lattice constant decreases with increase in Cr^{3+} composition.
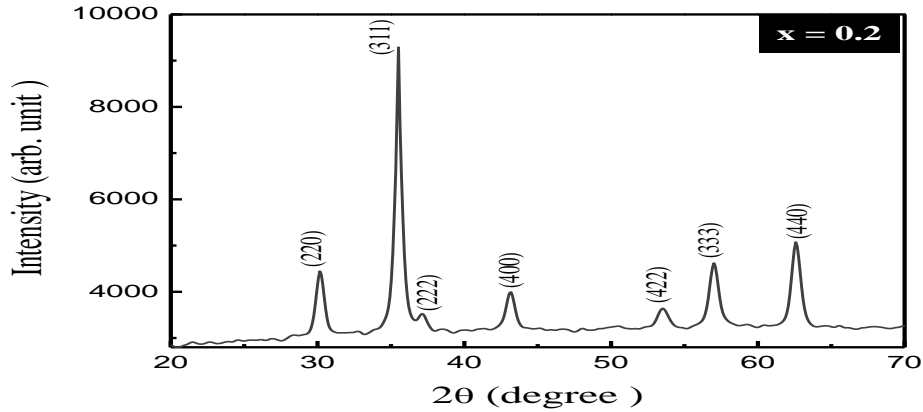
Fig. 2: Typical XRD pattern for samples x =0.2

IR Spectroscopy

A typical IR spectra of the chromium substituted copper nickel zinc ferrite system is shown in Figure 3. It is observed from Figure 3 that the higher frequency band (v_1) is observed around 575 cm^{-1}, assigned to stretching vibration of tetrahedral site; whereas lower frequency band (v_2) is observed around 400 cm^{-1} assigned to stretching vibration of octahedral site [10].
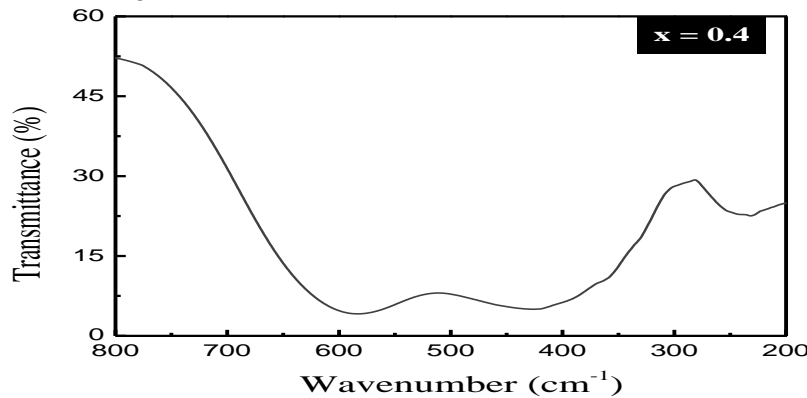

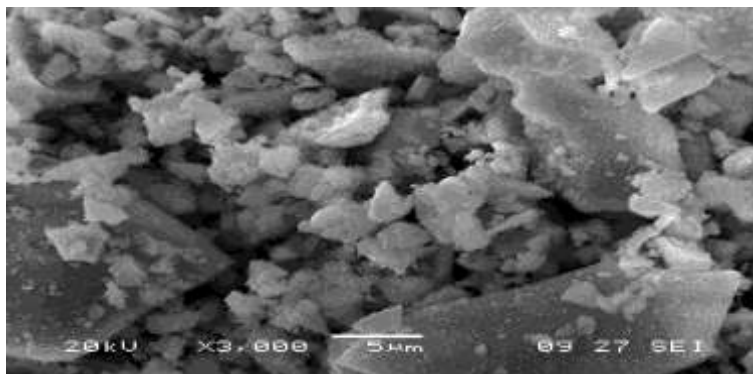**Fig. 3:** Typical IR spectrum for samples x =0.4

SEM and TEM

Fig. 4: Scanning electron micrograph for sample x = 0.2

Typical Scanning electron micrograph (SEM) of the surfaces of the chromium substituted copper nickel zinc ferrite system is shown in Figure 4 and typical Transmission electron micrograph (TEM) of

the surfaces of the sample is shown in Figure 5. It is observed from the SEM and TEM images that the prepared samples are amorphous and porous in nature.
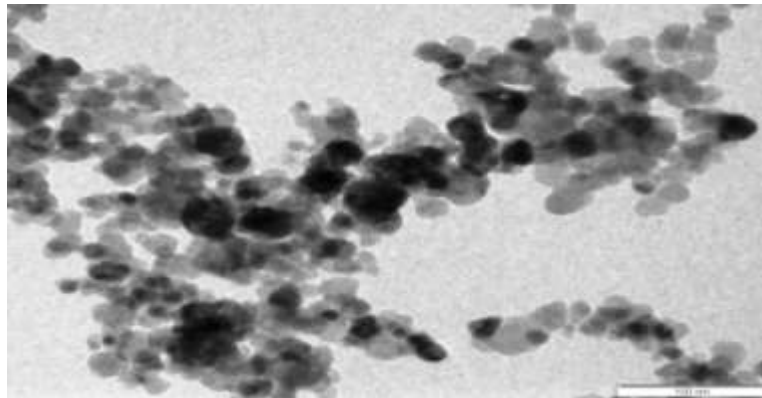

Fig. 5: Transmission electron micrograph for sample x = 1.0

Cation Distrubution

The cation distribution in spinel ferrite can be obtained from an analysis of the X-ray diffraction pattern. In the present work, the Bertaut method [11] is used to determine the cation distribution. The best information on cation distribution is achieved by comparing the experimental and calculated intensity ratios for reflections whose intensities (i) are nearly independent of the oxygen parameter, (ii) vary with the cation distribution in opposite ways and (iii) do not significantly differ. In the present work the ratio of (220)/(440) and (422)/(440) were used. The ratios of these planes are sensitive to cation distribution and are listed in Table 1.

The cation distribution for each concentration and the site preferences of cations distributed among the tetrahedral (A) and octahedral [B] sites are listed in Table 1. One can find the Zn^{2+} ions prefer to occupy the tetrahedron site (A sublattice) and both Ni^{2+} and Cu^{2+} ions mainly enter octahedron site (B sublattice). However, Fe^{3+} ions occupy both the available tetrahedral (A) and octahedral [B] sublattices. Cr^{3+} preferentially replaces Fe^{3+} from octahedral sites because of favorable crystal field effects ($Cr^{3+}6/5\Delta_0$, $Cr^{3+}0\Delta_0$) [11]. The data in Table 1 show that Cr^{3+} ions predominately occupy the octahedral sites, which is consistent with the preference for large octahedral site energy. With increasing Cr^{3+} content, the fraction Cr^{3+} ions in octahedral sites increases, whereas the fraction of Fe^{3+} ions in octahedral sites decreases linearly.
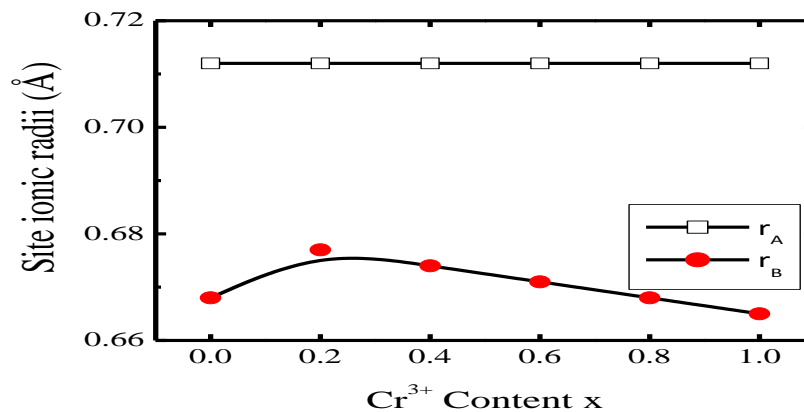

Fig. 6: Variation of site ionic radii (r_A and r_B) with Cr^{3+} substitution

The mean ionic radius of the tetrahedral A- and octahedral B-sites (r_A and r_B) was calculated [12, 13]. It is observed that radius of tetrahedral site 'r_A' remains constant at (0.712 Å) whereas radius of octahedral site 'r_B' decreases with increasing Cr^{3+} substitution (Table 2 and Figure 6). The decrease in r_B is due to the increasingly high occupation of the B site by the smaller ionic radius of Cr^{3+} (0.64 Å) ions that replacing Fe^{3+} (0.67 Å) ions.

Table 1: Cation distribution and intensity ratios

Comp 'x'	Cation distribution	Intensity ratio			
		$I_{(220)}/I_{(400)}$		$I_{(422)}/I_{(440)}$	
		Obs.	Cal.	Obs.	Cal.
0.0	$(Zn_{0.6}Fe_{0.4})$ $[Ni_{0.2}Cu_{0.2}Fe_{1.6}]$	1.7416	1.2006	0.2704	0.7000
0.2	$(Zn_{0.6}Fe_{0.4})$ $[Ni_{0.2}Cu_{0.2}Fe_{1.4}Cr_{0.2}]$	1.7638	1.0897	0.2759	0.7196
0.4	$(Zn_{0.6}Fe_{0.4})$ $[Ni_{0.2}Cu_{0.2}Fe_{1.2}Cr_{0.4}]$	1.9719	1.1452	0.2914	0.7258
0.6	$(Zn_{0.6}Fe_{0.4})$ $[Ni_{0.2}Cu_{0.2}Fe_{1.0}Cr_{0.6}]$	1.9922	1.1648	0.2954	0.7364
0.8	$(Zn_{0.6}Fe_{0.4})$ $[Ni_{0.2}Cu_{0.2}Fe_{0.8}Cr_{0.8}]$	2.0675	1.1098	0.2952	0.7908
1.0	$(Zn_{0.6}Fe_{0.4})$ $[Ni_{0.2}Cu_{0.2}Fe_{0.6}Cr_{1.0}]$	1.8907	1.0773	0.3022	0.8286

The theoretical values of lattice constant (a_{th}) were calculated by following equation [14]:

$$a_{th} = \frac{8}{3}\sqrt{3}\left[(r_A + R_0) + \sqrt{3}(r_B + R_0)\right] \qquad (1)$$

where r_A and r_B are radii of tetrahedral (A) site and octahedral [B] site, R_O is radius of oxygen ion (1.32 Å). The values of the theoretical lattice parameters for the different substitution level of Cr^{3+} ions is given in Table 2 and its variation is shown in Figure 7. The theoretical lattice constant decreased from 8.462 Å (x = 0.0) to 8.422 Å (x = 1.0) with the Cr^{3+} substitution.
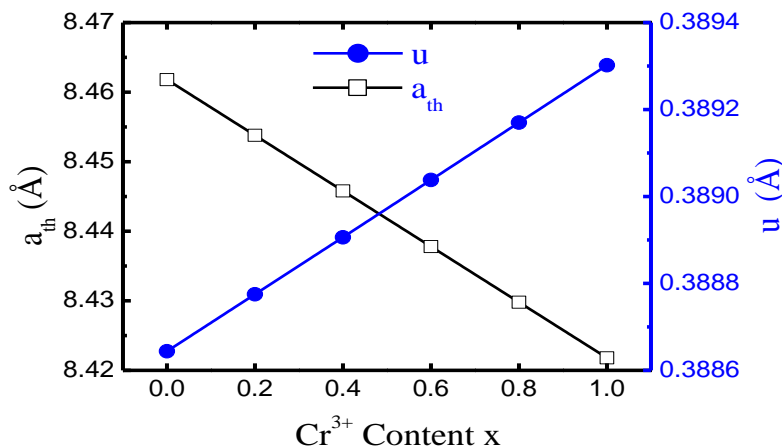

Fig. 7: Variation of theoretical lattice constant 'a_{th}' and oxygen positional parameter 'u' with Cr^{3+} substitution

The oxygen positional parameter 'u' was calculated using the following equation [14]:

$$u = \left[(r_A + R_0)\frac{1}{\sqrt{3}a} + \frac{1}{4}\right] \qquad (2)$$

where 'a' is lattice constant, 'R_O' is the radius of oxygen ion (1.32 Å) and 'r_A' is the radius of tetrahedral A-site. In most oxidic spinels the oxygen ions are apparently larger than the metallic ions, and in spinel like structure the oxygen parameter has a value of about 0.375 for which the arrangement of O^{2-} ions equals exactly a cubic closed packing, but in actual spinel lattice this ideal pattern is slightly deformed. For a given spinel compound, the anion sublattice expands or contracts on varying oxygen parameter until the tetrahedral and the octahedral site volumes match the radii of the constituent cations. As observed from Table 2 and Figure 4 that the u increased from 0.3886 Å to 0.3893 Å with the substitution of Cr^{3+} ions in NiCuZn ferrite. Little higher value of obtained u is due to a small displacement of the anions with the expansion of the tetrahedral interstices 'r_A'.

Table 2: Lattice Ionic radii r_A and r_B and theoretically lattice constant of system

Composition 'x'	r_A (Å)	r_B (Å)	a_{th} (Å)	u (Å)
0.0	0.712	0.668	8.462	0.3886
0.2	0.712	0.677	8.454	0.3888
0.4	0.712	0.674	8.446	0.3889
0.6	0.712	0.671	8.438	0.3890
0.8	0.712	0.668	8.431	0.3892
1.0	0.712	0.665	8.422	0.3893

The allied parameters such as tetrahedral and octahedral bond length (d_{Ax} and d_{Bx}), tetrahedral edge, shared and unshared octahedral edge (d_{AXE}, d_{BXE} and d_{BXEU}) were calculated:

$$d_{AX} = a\sqrt{3}\left(u - \frac{1}{4}\right) \tag{3}$$

$$d_{BX} = a\left[3u^2 - \left(\frac{11}{4}\right)u + \frac{43}{64}\right]^{\frac{1}{2}} \tag{4}$$

$$d_{AXE} = a\sqrt{2}\left(2u - \frac{1}{2}\right) \tag{5}$$

$$d_{BXEshaired} = a\sqrt{2}\left(1 - 2u\right) \tag{6}$$

$$d_{BXEunshaired} = a\left(4u^2 - 3u + \frac{11}{16}\right)^{\frac{1}{2}} \tag{7}$$

where 'a' is the experimental values of lattice constant and 'u' is oxygen positional parameter.

The values are presented in Table 3, which indicates that the tetrahedral and octahedral bond lengths decreases as Cr^{3+} ion substitution increases. The tetrahedral edge and shared and unshared octahedral edges decrease with Cr^{3+} substitution and may be due to the comparatively smaller ionic radii of Cr^{3+} as compared to Fe^{3+} ions.

Table 3: Tetrahedral bond (d_{AX}), octahedral bond (d_{BX}), tetra edge (d_{AXE}) and octa edge (d_{BXE})

Composition 'x'	d_{AX} (Å)	d_{BX} (Å)	Edges		
			Tetra edge	Octa edge	
			d_{AXE} (Å)	Shared d_{BXE} (Å)	Unshared d_{BXEU} (Å)
0.0	1.9102	2.0554	3.1193	2.8335	2.9781
0.2	1.9096	2.0547	3.1183	2.8326	2.9772
0.4	1.9075	2.0525	3.1149	2.8296	2.9739
0.6	1.9047	2.0494	3.1102	2.8253	2.9695
0.8	1.9037	2.0484	3.1087	2.8239	2.9680
1.0	1.8987	2.0429	3.1004	2.8164	2.9601

Conclusions

In the $Cu_{0.2}Ni_{0.2}Zn_{0.6}Fe_{2-x}Cr_xO_4$ system Zn^{2+} ions prefer to occupy the tetrahedron site (A sublattice) and both Ni^{2+} and Cu^{2+} ions mainly enter octahedron site (B sublattice). However, Fe^{3+} ions occupy both the available tetrahedral (A) and octahedral [B] sublattices. Cr^{3+} ions predominately occupy the octahedral sites. With increasing Cr^{3+} content, the fraction Cr^{3+} ions in octahedral sites increases, whereas the fraction of Fe^{3+} ions in octahedral sites decreases linearly. The value of u increased from 0.3886 Å to 0.3893 Å with the substitution of Cr^{3+} ions in NiCuZn ferrite.

References

[1] Carter, C. B., & Norton, M. G., *Ceramic materials: science and engineering*. Springer Science & Business Media. (2007).

[2] Lal, R., Sharma, N. D., Taneja, S. P., & Reddy, V. R., *Ind. J. Pure and Appl. Phys.,* 2007, 45, 231.

[3] Shinde, B. L., & Lohar, K. S., *Asian Journal of Research in Chemistry*, 2017, *10*(5), 621-625.

[4] Singhal, S., Barthwal, S. K., & Chandra, K., *Journal of magnetism and magnetic materials*, 2006, *296*(2), 94-103.

[5] Pandit, A. A., Shitre, A. R., Shengule, D. R., & Jadhav, K. M., *Journal of materials science*, 2005, *40*(2), 423-428.

[6] Shinde, B. L., Dhale, L. A., Ganure, K. A., & Lohar, K. S., *Asian Journal of Chemistry,* 2017, 29(11), 2531-2535.

[7] Singhal, S., Singh, J., Barthwal, S. K., & Chandra, K., *Journal of Solid State Chemistry*, 2005, *178*(10), 3183-3189.

[8] Joseyphus, R. J., Narayanasamy, A., Shinoda, K., Jeyadevan, B., & Tohji, K., *Journal of Physics and Chemistry of Solids*, 2006, *67*(7), 1510-1517.

[9] Hastings, J. M., & Corliss, L. M. *Physical Review*, 1956, *104*(2), 328.

[10] Shinde, B. L., Dhale, L. A., Suryavanshi, V. S., & Lohar, K. S., *Acta Chimica Slovenica*, 2017, *64*(4), 931-937.

[11] Weil, L., Bertaut, F., & Bochirol, L., *Journal de Physique et le Radium*, 1950, *11*(5), 208-212.

[12] Amer, M. A., *Hyperfine interactions*, 2000, *131*(1), 29-42.

[13] Yousif, A. A., Elzain, M. E., Mazen, S. A., Sutherland, H. H., Abdalla, M. H., & Masour, S. F., *Journal of Physics: Condensed Matter*, 1994, *6*(29), 5717.

[14] R. Valenzuela, *Magnetic ceramics*, Cambridge University Press, (1994).